Study of Dispersive and Anisotropic Scatterers Behavior in Radar Imaging Using Time-Frequency Analysis and Polarimetric Coherent Decomposition

Mickaël Duquenoy*†, Jean Philippe Ovarlez* Laurent Ferro-Famil†, Luc Vignaud* and Eric Pottier†

*Signal Processing Unit, Electromagnetism and Radar Department (DEMR)
ONERA, Palaiseau, France
Chemin de la Hunière, F-91761 Palaiseau cedex
Telephone: (+33) 1 69 93 62 95, Fax: (+33) 1 69 93 62 69
Email : mickael.duquenoy@onera.fr, ovarlez@onera.fr, vignaud@onera.fr

†Image and Remote Sensing Group, Institute of Electronics and Telecommunications from Rennes (IETR)
University of Rennes 1, Rennes, France
Campus Beaulieu, Bat 11D, 263 avenue Général Leclerc, CS-74205 Rennes cedex
Telephone: (+33) 2 23 23 67 14, Fax: (+33) 2 23 23 69 63
Email : laurent.ferro-famil@univ-rennes1.fr, eric.pottier@univ-rennes1.fr

***Abstract*— A fully polarimetric Time-Frequency Analysis is proposed for Radar Imaging (SAR, ISAR) to analyse the anisotropic and dispersive behavior of deterministic target illuminated by a radar sensor. This method is based on the hyperimage concept which describes the response of scatterers as a function of the observation angle, of the emitted frequency and of the polarimetric decomposition. New polarimetric hyperimages point out a non-stationary behavior which can be interpreted by the physics parameters of the target (geometrical shape, relative orientation). They allow a best understanding of the scattering mechanisms. Basic statistics extracted from these representations show that they are tools to detect non-stationnary scatterers and are the first step to a new classification.**

I. Introduction

Conventional Radar Imaging assumes that all the scatterers are considered as bright points (isotropic for all the directions of presentation and white in the frequency band). Recent studies based on the use of time-frequency analysis allowed to describe the angular and frequency behavior of the spatial distribution of all the image scatterers and shown that some scatterers were not isotropic and white. This is the case for example for modern high resolution SAR sensors with wide bandwidth and wide azimut beam width. In this paper, a fully polarimetric time-frequency analysis method is proposed to extend these analyses with polarimetric radars. This technique decomposes processed polarimetric radar images into frequency/angular/polarization information of the image scatterers (called hyperimage). It allows to detect non-stationary time-frequency polarimetric behaviors in the image and may be of great utility for target recognition and classification.

II. Classical Radar Image Formation

The backscattering coefficient $H(\vec{k})$ for a given object illuminated by a radar is characterized, for a distance R going to infinity, as the ratio between the incoming field E_r and the emitted field E_i (spherical waves) :

$$\left|H(\vec{k})\right| = \lim_{R\to\infty} \sqrt{4\pi R^2}\,\frac{E_r}{E_i}. \tag{1}$$

The squared modulus of $H(\vec{k})$ is called the Radar Cross Section (RCS) of the object for the wave vector $\vec{k}$ and is expressed in squared meter. Wave vector $\vec{k}$ is related to the frequency f and to the direction θ of illumination by $\left|\vec{k}\right| = 2f/c$ and $\theta = \arg(\vec{k})$ (see figure 1 for the geometry of SAR imaging).

The model usually used in radar imaging is the model of bright points [1]. The object under analysis can be seen as a set of bright points, i.e. a set of independent sources which reflect in the same way for all frequencies (white points) and all directions of presentation (isotropic points). Let $I(\vec{r})$ be the amplitude of the bright point located in $\vec{r} = (x, y)^T$ in a set of cartesian axes related to the object. Under far field conditions (decomposition into planes waves), the complex backscattering coefficient for the whole object is then given by the in-phase summation of each reflector contribution :

$$H(\vec{k}) = \int I(\vec{r})\, e^{-2i\pi\vec{k}.\vec{r}}\, d\vec{r}. \tag{2}$$

After a Fourier Transform of (2), one can obtain the spatial repartition $I(\vec{r})$ of the reflectors for a mean frequency (the center frequency) and for a mean angle of presentation :

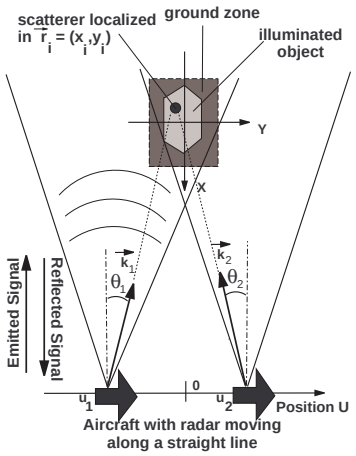

Fig. 1. *A reflector, viewed at two different angles of presentation and at two different frequencies in SAR-stripmap mode*

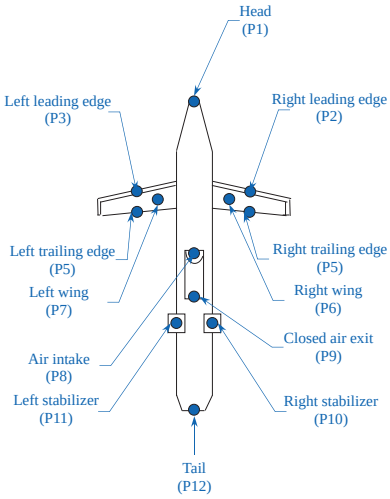

Fig. 2. *Aircraft scaled model used for simulation in anechoic chamber*

$$I(\vec{r}) = \int H(\vec{k})\, e^{2i\pi\vec{k}.\vec{r}}\, d\vec{k}. \tag{3}$$

It can be noted that any imaging operation working with the above set of data will permit only to localize the projections of the bright points on the measurement plane (slant plane).

For the aircraft scaled model under study presented in figure 2 and analysed in anechoic chamber, figure 3 shows its backscattering coefficient $H(\vec{k})$ and the spatial repartition of its reflectors. The spatial image shows the location of the target bright points but does not allow to characterize their frequency and angular behavior. Next section will now present a method which allows to characterize these missing informations.

III. 2D Time-Frequency Analysis and Hyperimage Concept

When an object is illuminated by a broad-band signal and/or for a large angular extent, it is realistic to consider that the amplitude spatial repartition $I(\vec{r})$ of the reflectors depends

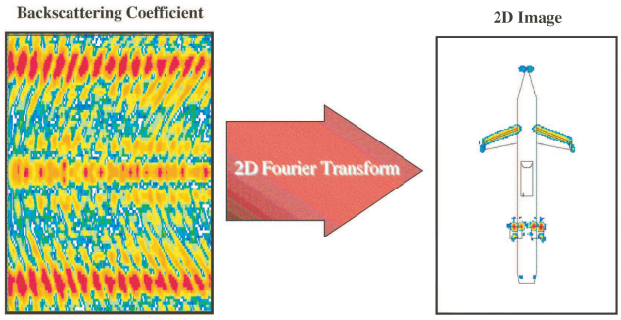

Fig. 3. *Classical bi-dimensional radar imaging of aircraft scaled model*

on frequency f and on aspect angle θ. This repartition depending on the wave vector $\vec{k}$, it will be noted in the following by $I(\vec{r}, \vec{k})$.

The quantity $I(\vec{r}, \vec{k})$ represents the energy distribution of the backscattering coefficient $H(\vec{k})$ in the hyperplane $(\vec{r}, \vec{k})$ and characterizes an "extended image" relative to the spatial repartition $I(\vec{r})$. Such images can be built with classical Time-Frequency Distributions (TFD) [2], [3] extended to two-dimensions and are called hyperimages.

It is well known that some TFD (Cohen Class and Affine Class) are generally bilinear energy distributions which do not allow to conserve the phase of the signals and which generate some interferences between components in the time-frequency plane. For these reasons, they cannot be of any help for polarimetric analysis. These drawbacks are avoided by using the Multidimensional Continuous Wavelet Transform (MCWT) [4], [5], [8], [6], [7]. This allows to define the hyperimage $I(\vec{r}_0, \vec{k}_0)$ as the squared modulus of the wavelet coefficient $C_H(\vec{r}_0, \vec{k}_0)$ defined by :

$$C_H(\vec{r}_0, \vec{k}_0) = \int H(\vec{k})\, \Psi^*_{\vec{r}_0, \vec{k}_0}(\vec{k})\, d\vec{k}\,, \tag{4}$$

where $\Psi_{\vec{r}_0, \vec{k}_0}(\vec{k})$ is a family of wavelet bases generated from the mother wavelet $\phi(k, \theta)$ localized around $(k, \theta) = (1, 0)$ and positioned spatially at $\vec{r} = \vec{0}$ according to :

$$\Psi_{\vec{r}_0, \vec{k}_0}(\vec{k}) = \frac{1}{k_0}\, e^{-2i\pi\vec{k}.\vec{r}_0}\, \phi\left(\frac{k}{k_0}, \theta - \theta_0\right). \tag{5}$$

The quantity $I(\vec{r}_0, \vec{k}_0)$ is, in fact, the energy distribution of the reflected signal $H(\vec{k})$ in the hyperplane $(\vec{r}_0, \vec{k}_0)$:

$$I_H(\vec{r}_0, \vec{k}_0) = \left| \frac{1}{k_0} \int H(\vec{k})\, e^{2i\pi\vec{k}.\vec{r}_0}\, \phi\left(\frac{k}{k_0}, \theta - \theta_0\right) d\vec{k} \right|^2 \tag{6}$$

Since the wavelet coefficients are complex, the phase of the hyperimage is always conserved and can be used for polarimetric analysis. The wavelet coefficient can be more simply interpreted in SAR imaging as a multi-look analysis in angular domain and as subband decomposition in spectral

domain. Figure 4 shows this kind of analysis. The MCWT of the backscattering coefficient allows to give, for each scatterer, its spectral and angular behavior. The image shows that some scatterers have different frequency responses (colored scatterers) and different responses in angular domain (anisotropic scatterers). For example, the head of the target is assimilated to a sphere which is considered, in high frequency, as a non-dispersive and isotropic element : in the figure, the response of the head is uniform and constant in the angle/frequency plane. On the contrary, the left and right wings show two different angle/frequency responses.

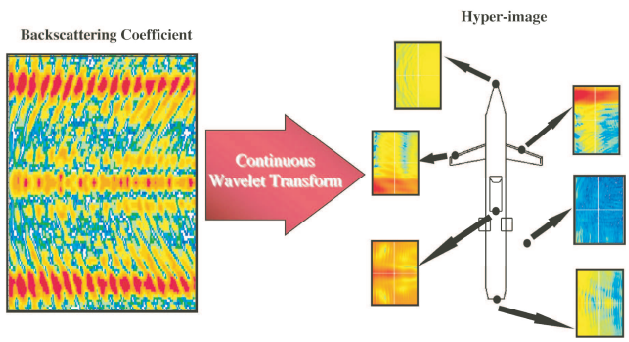

Fig. 4. *Extended bi-dimensional radar imaging of aircraft scaled model*

In the next section, the Polarimetric Coherent Decomposition methods will be briefly recalled and will be extended to the hyperimage concept.

IV. Polarimetric Coherent Decomposition and Polarimetric Hyperimage Concept

A. Conventional Polarimetric Coherent Decomposition

A full polarimetric radar is generally designed to transmit and receive microwave radiation which is horizontally polarized (H) or vertically polarized (V). The polarimetric generalization of the scattering coefficient is called the scattering matrix. For each location of a scatterer, this matrix is composed of 4 complex numbers, representing the complex scattering coefficients for all four polarization combinations, hH, hV, vH and vV (capital letters indicate the transmit wave polarization and small letters the received polarization).

$$[S](\vec{r}) = \begin{pmatrix} I_{H_{\mathrm{hH}}}(\vec{r}) & I_{H_{\mathrm{hV}}}(\vec{r}) \\ I_{H_{\mathrm{vH}}}(\vec{r}) & I_{H_{\mathrm{vV}}}(\vec{r}) \end{pmatrix} \tag{7}$$

The goal of the target decomposition theory is to decompose (please note that such a decomposition is generally not unique) the average scattering mechanism as the sum of N independent elements, in order to associate a simple physical mechanism with each of them :

$$[S](\vec{r}) = \sum_{k=1}^{N} [S]_k(\vec{r}) \tag{8}$$

The span is generally defined as the sum of the squared modulus of each element of the matrix :

$$\mathrm{SPAN}(\vec{r}) = |I_{H_{\mathrm{hH}}}(\vec{r})|^2 + |I_{H_{\mathrm{hV}}}(\vec{r})|^2 + |I_{H_{\mathrm{vH}}}(\vec{r})|^2 + |I_{H_{\mathrm{vV}}}(\vec{r})|^2$$

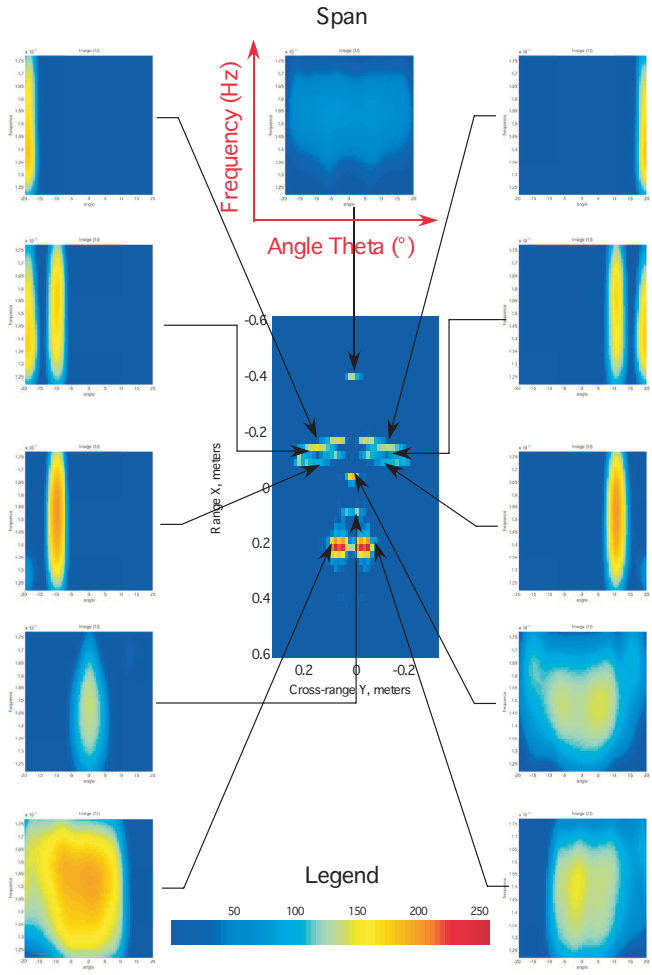

Fig. 5. *Span of the aircraft scaled model analysed between -20 and 20 degrees and for [12, 18] GHz*

In this paper we only investigate the well known coherent target decomposition (CTD) methods such Krogager [9] and Cameron [10]. These methods are generally applied on full resolution polarimetric images and hence, all physical mechanisms are totally averaged on the emitted frequency band and on the whole angular domain.

In the next sections, we show that, applying the CTD methods on the polarimetric hyperimages allows to describe the polarimetric contributions (Krogager) and the polarimetric nature (Cameron) of the scatterers for each frequency and the angle of presentation. These studies allow to follow the polarimetric evolution of the scatterers versus frequency and angle and show that the polarimetric information is generally dispersive and anistropic.

B. Extended Polarimetric Coherent Decomposition

The scattering matrix used for the CTD methods will now depend on frequency and on angle of presentation. It will be

defined in the following by :

$$\left[\tilde{S}\right](\vec{r},\vec{k}) = \begin{pmatrix} I_{H_{\mathrm{hH}}}(\vec{r},\vec{k}) & I_{H_{\mathrm{hV}}}(\vec{r},\vec{k}) \\ I_{H_{\mathrm{vH}}}(\vec{r},\vec{k}) & I_{H_{\mathrm{vV}}}(\vec{r},\vec{k}) \end{pmatrix} \tag{9}$$

The exended span is now defined as the sum of the squared modulus of each element of the scattering matrix $\left[\tilde{S}\right](\vec{r},\vec{k})$:

$$\begin{aligned} \mathrm{SPAN}(\vec{r},\vec{k}) &= \left|I_{H_{\mathrm{hH}}}(\vec{r},\vec{k})\right|^2 + \left|I_{H_{\mathrm{hV}}}(\vec{r},\vec{k})\right|^2 \\ &+ \left|I_{H_{\mathrm{vH}}}(\vec{r},\vec{k})\right|^2 + \left|I_{H_{\mathrm{vV}}}(\vec{r},\vec{k})\right|^2 \end{aligned} \tag{10}$$

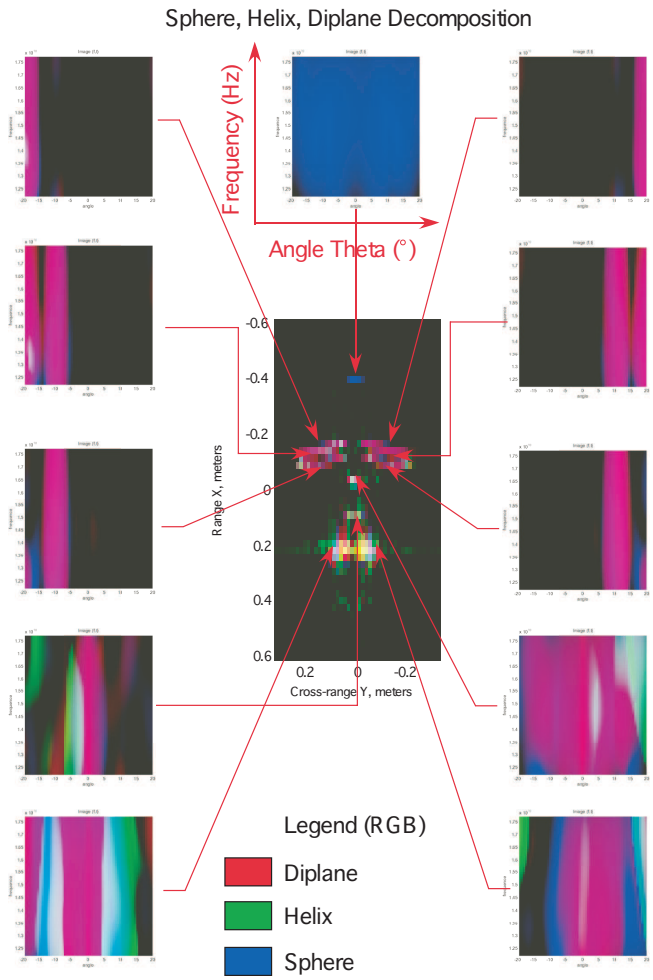

Fig. 6. *Krogager Decomposition of an aircraft*

V. Results on Experimental Data

Polarimetric hyperimages have been tested on full polarimetric data from anechoic chamber between $-25\,\mathrm{deg}$ and $25\,\mathrm{deg}$ degrees (only $[-20\,\mathrm{deg},\ 20\,\mathrm{deg}]$ are represented here) for a frequency band of [12, 18] GHz. The target is an aircraft scaled model called Cyrano (fig 2). Figure 5 characterizes the span evolution in the angle/frequency plane for each scatterers and shows that major of the scatterers are colored and anisotropic.

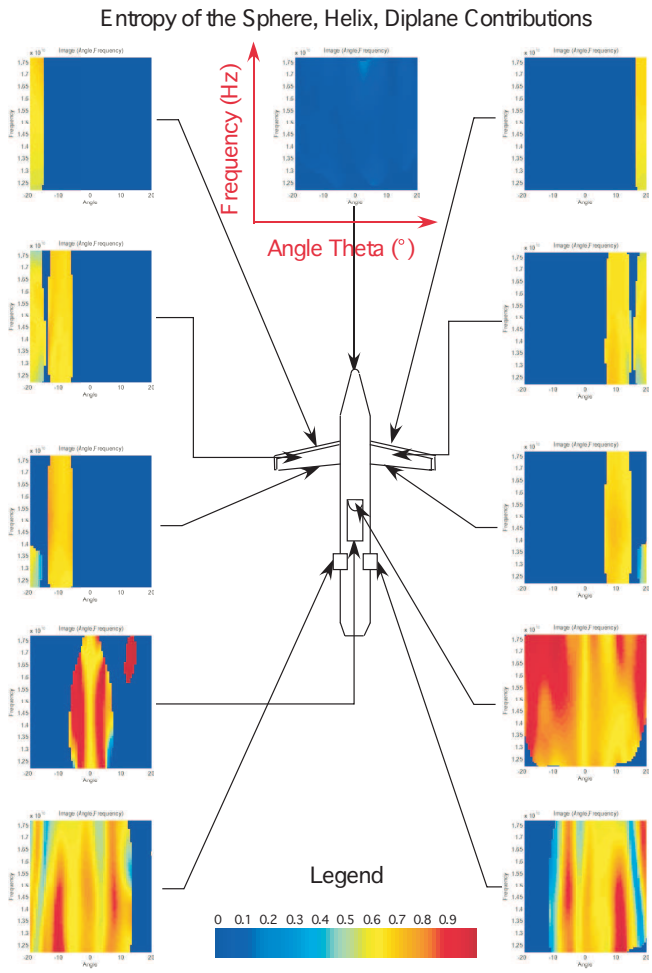

Fig. 7. *Entropy of Krogager contributions*

A. Krogager CTD : Sphere, diplane, helix decomposition

Krogager [9] has proposed to decompose the scattering matrix into a combination of the responses of a sphere, a diplane and a helix. Figure 6 illustrates the Krogager decomposition in the angle/ frequency domain. It shows the representation (RGB colors composition) of the polarimetric contributions (sphere, helix, diplane) of each element for each frequency and angle of presentation. The center image represents the spatial repartition of the scatterers at full resolution, the level representing Krogager decomposition. To enhance Krogager representation, figure 7 characterizes the entropy of the three Krogager contributions. Consider the right leading edge P2 (characterized by an inclinaison of 20 degrees in the horizontal plane) and the right trailing edge P5 (characterized by an inclinaison of 10 degrees in the horizontal plane) : the responses of P2 and P5 scatterers match perfectly with the geometry. P6 scatterer analysis (right wing) shows a mix of these two contributions which is the consequence of the Heisenberg incertitude principle (choice of the angle and frequency widths of the mother wavelet).

B. Cameron CTD and Classification

The Cameron decomposition [10] performs a decomposition of the scattering matrix based on two properties of radar targets : symmetry and reciprocity. Contributions of the Cameron decomposition are : triedral, diplane, dipole, cylinder, narrow diplane and quater wave device. With this basis of decomposition, Cameron proposed a classification scheme which allows to give the polarimetric nature of the scatterers (left helix, right helix, asymetrical helix, triedral, dihedral, narrow dihedral, dipole, cylinder and quater wave device). It also allows to determine the Huynen [11] parameter Ψ which gives the orientation of the scatterers in the vertical plane (angle around the line of sight).

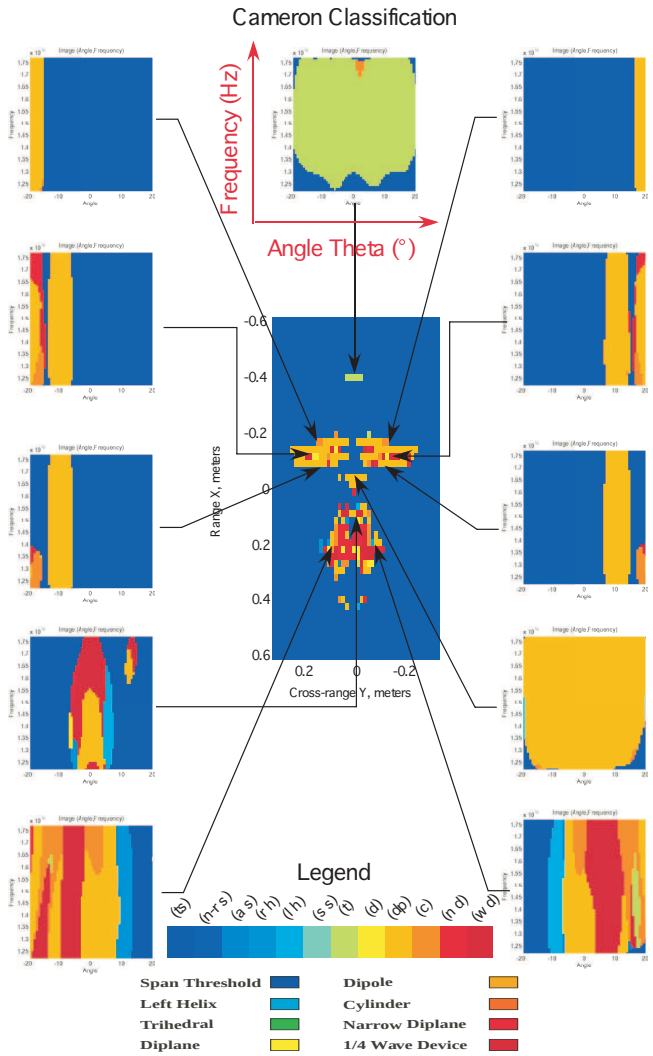

Fig. 8. *Cameron polarimetric classification*

Figure 8 shows the Cameron classification of the polarimetric nature of the scatterers relative to frequency and angle of presentation. The center image represents the spatial repartition of the scatterers at full resolution, the level representing the Cameron classification. The Cameron classification gives more information than Krogager decomposition. In particular, it shows that the nature of the trailing and leading edges is characterized here by a dipole. The head of the target is classified here as trihedral for each frequency and angle of presentation.

In figure 9, for the scatterers P2 P3 and P6, the Huynen parameter Ψ of the Cameron decomposition (angle around the line of sight) always shows a response (($\Psi = -90\,\mathrm{deg}$ for the right wing and $\Psi = 90\,\mathrm{deg}$ for the left wing) located in the angular plane for the orientation angle of $10\,\mathrm{deg}$. It can be simply explained by the fact that the aircraft wings are characterized by an elevation of $10\,\mathrm{deg}$ in the vertical plane.

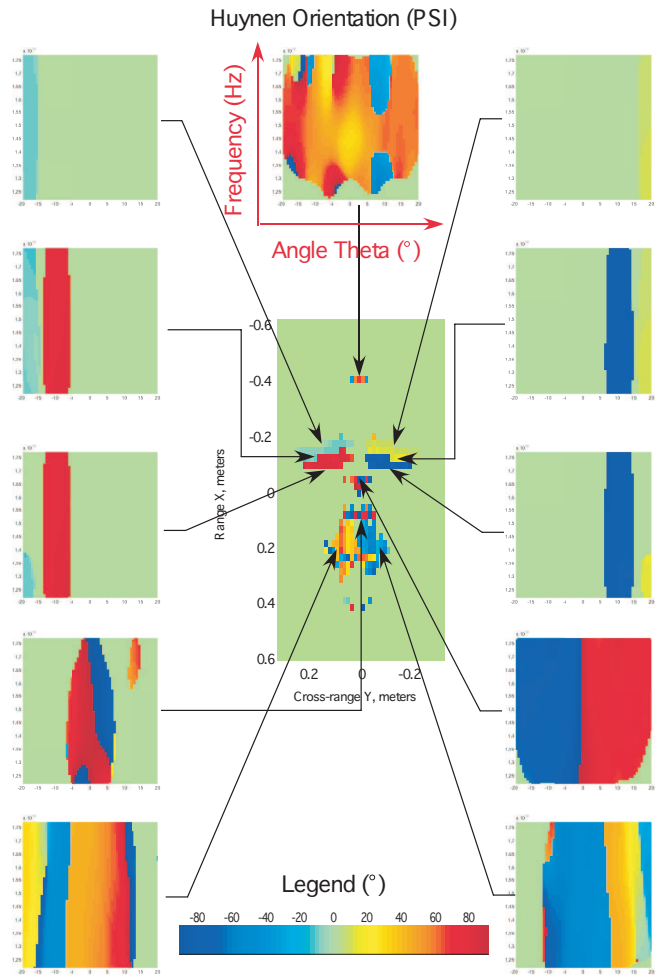

Fig. 9. *Distribution of the Huynen parameter Ψ in the Cameron decomposition*

VI. Conclusion

In this paper, we have jointly presented a time-frequency analysis and polarimetric coherent decomposition analysis which can be applied to highlight a polarimetric non-stationary behavior of the scatterers versus frequency and angle of presentation. It appears that the polarimetric response is dependent on the aspect angle from which the scatterers are

illuminated and on the emitted frequency. Non-stationarity can be explained by the shape of the scatterers, by their orientation, or by the limitations of the time-frequency analysis. Exploiting these informations allows to better understand the physical polarimetric mechanisms in order to improve targets recognition and classification in radar imaging (SAR, ISAR, ..).

AKNOWLEDGEMENTS

The authors wish to thank Anyl Cheraly and François Tardivel of ONERA, Palaiseau, France, for supplying the anechoic chamber data.

REFERENCES

[1] D.L. Mensa, *High Resolution Radar Imaging*, Artech House (1981), USA.

[2] L. Cohen, *"Time Frequency Distributions - A Review"*, Proc. of the IEEE, Vol.77, No.7, July 1989

[3] J. Bertrand P. Bertrand, *"A Class of Affine Wigner Functions with Extended Covariance Properties"*, J. Math Physics, Vol. 33, No. 7, pp. 2515-2517, 1992

[4] J. Bertrand P. Bertrand and J.P. Ovarlez, *"Frequency Directivity Scanning in Laboratory Radar Imaging"*, Int. J. of Imaging Systems and Technology, **5** (1994), 39-51.

[5] J.P. Ovarlez L. Vignaud J.C. Castelli M. Tria and M. Benidir, *"Analysis of SAR Images by Multidimensional Wavelet Transform"*, IEE-Radar, Sonar and Navigation- Special Issue On Time-Frequency Analysis for Synthetic Aperture Radar and Feature Extraction, Vol. **150**, No. (4), (august 2003), pp. 234-241.

[6] J. Bertrand, P. Bertrand, J. P. Ovarlez, *"Dimensionalized wavelet transform with application to radar imaging"*, IEEE-ICASSP, vol. 4, pp. 2009-2012, 14-17 April 1991.

[7] V. C. Chen, H. Ling, *"Time-frequency transforms for radar imaging and signal analysis"*, Artech House, 2002.

[8] J. Bertrand and P. Bertrand, *"The Concept of Hyperimage in Wide-Band Radar Imaging"*, IEEE Trans. Geosc. Remote Sensing, **34** (1996), 1144-1150.

[9] E. Krogager, Z.H. Czyz, *"Properties of the sphere diplane, helix decomposition"*, The Third International Workshop on Radar Polarimetry, vol. 1, p. 106-114, March 1995.

[10] W.L. Cameron, N.N. Youssef, L.K. Leung *"Simulated polarimetric signatures of primitive geometrical shapes"*, IEEE Trans.-on Geoscience and Remote Sensing, vol. 34, nr. 3, pp. 793-803, May 1996.

[11] J.R. Huynen, *"Measurement of the target scattering matrix"*, Proc. IEEE, vol. 53, pp. 936-946, Aug. 1965